Science of the Total Environment 905 (2023) 167186

Contents lists available at ScienceDirect

Science of the Total Environment

journal homepage: www.elsevier.com/locate/scitotenv

# Geochemical characterization of the Martian analogues Enekuri and Fruiz, located in the Basque-Cantabrian Basin, by spectroscopic techniques

Jennifer Huidobro [a,*], Patricia Ruiz-Galende [a], Imanol Torre-Fdez [a], Julene Aramendia [a], Jesús Martínez-Frías [b], Cristina García-Florentino [a], Leticia Gómez-Nubla [a], Kepa Castro [a], Gorka Arana [a], Juan Manuel Madariaga [a]

[a] Department of Analytical Chemistry, University of the Basque Country UPV/EHU, Barrio Sarriena, P.O. Box 644, E-48940 Leioa, Biscay, Spain
[b] Instituto de Geociencias, IGEO (CSIC,UCM), C/ Doctor Severo Ochoa, 7. Entre pabellones Building 7 and 8, 4th floor, E-28040 Madrid, Spain

## HIGHLIGHTS

- Geochemical characterization of the Enekuri and Fruiz Martian analogues
- Using VNIR, Raman and XRF spectroscopies, as they are in future planetary missions
- The presence of chlorite is an evidence of initial aqueous activity.
- Inland outcrops weathering are characterized by biological activity.

## GRAPHICAL ABSTRACT

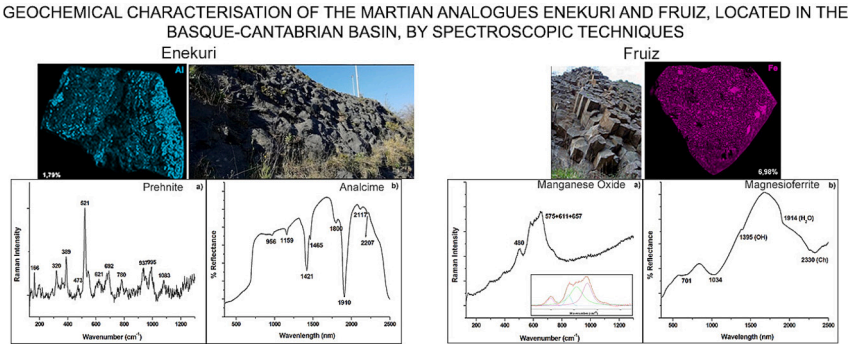


## ARTICLE INFO

Editor: Damia Barcelo

*Keywords:*
Martian analogue
Raman spectroscopy
VNIR spectroscopy
XRF spectroscopy
Volcanic
Basque-Cantabrian Basin

## ABSTRACT

This work presents the geochemical characterization of two Martian analogues located in the Basque-Cantabrian Basin: Enekuri and Fruiz. In contrast to previous works carried out on the coastline analogues Meñakoz and Armintza (Biscay, Spain), these new outcrops are not in contact with sea-water nowadays. Hence, the weathering processes observed in Enekuri and Fruiz (inland) are different from those observed in Armintza and Meñakoz (coastline). In this way, among all the mineral phases found the only ones in common between inland and coastline outcrops are albite and chlorites, minerals that were formed in aqueous conditions. Understanding the differences presented in both types of outcrops could help to interpret the future results from the missions Mars2020 and the ExoMars2022, since coastline outcrops are affected by sea-water weathering and inland outcrops are altered by the high biological activity.

* Corresponding author.
*E-mail address:* jennifer.huidobro@ehu.eus (J. Huidobro).

https://doi.org/10.1016/j.scitotenv.2023.167186
Received 10 August 2023; Received in revised form 15 September 2023; Accepted 16 September 2023
Available online 19 September 2023

## 1. Introduction

One of the main objectives of the NASA's mission, Mars 2020, and the ESA's mission, ExoMars 2022, is to find life evidences and to demonstrate the potential habitability of the red planet. For that purpose, minerals associated to the presence of water are of high importance for the selection of those landing sites (Vago et al., 2017). Moreover, some of these minerals, which need water for their formation (phyllosilicates, among others), arise from weathering processes of igneous rocks. Therefore, knowing the hydrated mineral phases on Mars, the mineralogical history of the Martian surface can be inferred.

Previous Mars space missions, like The Viking Project, showed the importance of volcanic processes in the history of Mars. Most of the ancient Martian crust is certainly of magmatic origin (volcanic and plutonic). However, the heavy impact bombardment, together with aeolian and aqueous geological processes have modified the primary landforms such as flows and structures which might be vents (Head, 2007). Therefore, the current Martian surface is characterized by extensive volcanic activity, not uniformly distributed, that includes several volcanic landforms, such as domes or plains. That diversity of landforms implies different eruption styles, changes in the style of volcanism with time and the interaction with the Martian atmosphere during the evolution of Mars (Werner, 2009).

The landing sites for the NASA's and ESA's missions are Jezero Crater an Oxia Plamun respectively. On the one hand, Jezero Crater is a Noachian crater that likely contained a paleolake and deltas. It is located on the inner ring of the Isidis Basin and impacted into basement materials interpreted to be Isidis ejecta. The presence of carbonates in a variety of depositional settings contrast with Hesperian sites like Meridiani and Gale crater, which are influenced by sulfate minerals. The Jezero impact likely predates the regional olivine unit, placing the impact in the Noachian (Goudge et al., 2015). On the other hand, Oxia Planum is located in the Chryse Planitia region in Oxia Palus area. Here, the diversity in geological features indicates active geological processes being one of the most studied areas on Mars. Oxia Planum belongs to the southern lowlands, which are Noachian age terrains. Many output channels dissect the zone and converge to Chryse Planitia (Reyes Ayala, 2016). Most of the minerals related with the possible presence of water, and, hopefully, potential biosignatures, have been predominantly identified in Noachian terrains and it is one of the reasons why these landing sites were chosen.

The exploration of Mars is largely based on comparisons with Earth analogue environments and processes (Sutter et al., 2007). Therefore, in this research work some volcanic outcrops, Enekuri and Fruiz in the Basque-Cantabrian Basin (Northern Spain), have been analyzed. In this sense, by studying these samples possible similarities between Earth and its neighbor planet can be stablished.

In addition, this work aims to compare the Fruiz and Enekuri samples with other Basque-Cantabrian emplacements such as the Meñakoz (Torre-Fdez et al., 2021) and the Armintza outcrops (Ruiz-Galende et al., 2021). Since the environment in which these last outcrops are located differs from that of the emplacements studied in this work, it was supposed that the weathering processes observed would be different, and therefore, the mineralogical composition might be also different. Moreover, some differences were expected between Enekuri and Fruiz due to the different plate in which they are located and the different geological formation of the outcrop as described below.

The Basque-Cantabrian Basin (BCB) has undergone a long evolution process since Permian times. During these 250 My significant variations have taken place. It is commonly accepted that the BCB is the result of a complex evolution process including significant variations in the dominant tectonic regime (extension, transgression, compression), in the distance to the active plate boundary (rift, passive margin, active margin), and in the type of underlying crust (continental, transitional, hyperextended) (Robles et al., 2014).

Today, the BCB is a large sedimentary basin that was developed on the thinned continental crust between the European and Iberian plates during the Cretaceous period. It constitutes the western extension of the Pyrenean folded belt along extensive onshore areas of central-northern Spain and offshore areas of the Bay of Biscay. The Cretaceous succession of the BCB was initiated by Latest Jurassic rifting of the Iberian and European plates to create the Bay of Biscay. This rifting resulted in the break-up of the Jurassic carbonate ramps and the emergence and erosion of former marine areas. The boundary between the Iberian and European plates probably lies in the faulted area of the Biscay synclinorium and its associated submarine volcanism from the Late Albian onwards, which has been considered as the western continuation of the north Pyrenean fault zone (Martín-Chivelet et al., 2002). The northeast of Iberia underwent an important geodynamic event linked to ocean-floor spreading in the north Atlantic: the V-shaped Bay of Biscay opened leading to the separation of Iberia with respect to Europe. The Cretaceous magmatism in the NE Iberia has traditionally been related to the opening of the Bay of Biscay and allied rotation of the Iberia (Ubide Garralda, 2013). Geological and subsurface studies have enabled the subdivision of the Cretaceous tectonosedimentary evolution of the basin into a multiphase rifting stage (mainly early Cretaceous) and a post-rift stage (Late Cretaceous). The later one, was accompanied by intensive alkaline within-plate volcanism (Late Albian-Santonian) occurring on thinned continental crust along the fault systems that formed the plate boundary. This magmatism started in the NW before extending SE in the Biscay synclinorium (Martín-Chivelet et al., 2002).

During this period and along the BCB, the volcanism has many examples. In the pre-Aptian, Villaro formation, located towards the center of the basin, spilitic basaltic rocks interstratified with black mudstones have been described. Volcanoclastic sediments of Aptian age included in black mudstones have been also reported near Bilbao, in the Arrigorriaga area. In Early Albian, volcanoclastic and subvolcanic rocks from highest part of the volcanic edifice are present in the Mañaria and Larrano areas. Finally, thick volcanic units corresponding to the Late Albian can be found in areas such as Enekuri, and many others along the North-Biscay Anticlinorium. Since the Late Albian to Santonian magmatism, the rocks are described as submarine lavas, volcanoclastic beds and basic intrusions, predominantly basalts and trachytes with mineralogy and chemical composition typically alkaline (García-Mondéjar et al., 2019). The most important volcanic rocks in Biscay are: trachytes which are in volcanic cones formed by acid eruptions, andesites which can form mountains and are composed by plagioclases, pyroxenes and biotites, and basalts which are similar to the previous ones (Gómez Tejedor, 1976).

Considering volcanic activity happened on Mars, and the existence of water in some periods of its history, it could be possible that some episodes of submarine volcanism took place. Therefore, the study of this type of scenario is of high importance since they have not been widely studied and could be considered as Martian analogues. For that purpose, spectroscopic techniques similar to the ones implemented in the Mars2020 and ExoMars2022 rovers, have been used for the geochemical characterization of the samples collected in the mentioned emplacements.

## 2. Materials and methods

### 2.1. Geological setting

The volcanic rocks of Enekuri (43°29′67.07″N, 2°95′16.17″W, Fig. S1) are in the Iberian margin and were formed in the Late Albian. They appear controlled by the NW-SE set of faults that constitute the Bilbao fault zone (García-Mondéjar et al., 2019).

The outcrops located in this area are from the Upper Cretaceous and are situated in the north part of the Bilbao anticlinorium. Here, materials from volcanic origin are interbedded with fine sediments, lutites and marls. Among the volcanic materials, the presence of a basaltic flow and pillow lavas is highlighted. The presence of sandstones and shales before

the volcanic sequence evidences the instability associated with the volcanic processes (Badillo et al., 1987).

The Fruiz outcrop (43°19′53.68″N, 2°47′28.90″W, Fig. S2) belongs to the Gernika-Elgoibar fault in the European margin to the northeast of Bilbao. The Gernika-Elgoibar fault is separated from the Bilbao fault by the Late Cretaceous-Tertiary Biscay synclinorium. The volcanic rocks of Gernika-Elgoibar fault zone were dated as Late Albian-Santonian (as Meñakoz) and therefore, the outcrops from this fault coincided with the youngest eruptions of the Bilbao fault. This episode is the most important one due to its extension, facies diversity and internal volcanic sequences (Castañares et al., 1997).

The Elgoibar fault is considered the western expression of the North Pyrenean fault. Stratigraphic and sedimentology data suggest that the Elgoibar fault was left lateral and it controlled the development of the depositional system during the Aptian-Albian and the Late Cretaceous (Agirrezabala and García-Mondéjar, 2001).

Fruiz is the best example of the columnar disjunction feature. At this point, several outcrops of this type appear, being two of them superposed. The prisms exhibit a pentagonal basement of up to 60 cm of side. A succession of sedimentary, volcanic and pyroclastic events can be observed (Cuevas et al., 1981).

### 2.2. Instrumentation

The Fruiz and Enekuri samples were elementally and molecularly characterized. On the one hand, for the elemental characterization μ-energy dispersive X-ray fluorescence (μ-EDXRF) spectroscopy was used. On the other hand, for the molecular characterization X-ray diffraction (XRD), Raman and visible near infrared (VNIR) spectroscopies were used.

#### 2.2.1. The μ-EDXRF spectrometer

The elemental characterization of the samples was performed by using both single point analysis and hyper map capabilities of the μ-EDXRF spectrometer M4 Tornado (Bruker Nano GmbH, Berlin, Germany). This instrument has a micro-focus side window Rh tube powered by a low-power HV generator and cooled by air that extends to a maximum current of 700 μA and voltage of 50 kV. It implements an X-Flash silicon drift detector with 30 $mm^2$ sensitive area and energy resolution of 145 eV for Mn-Kα. The micrometric lateral resolution of the instrument, 25 μm for the Mo Kα-line, is achieved thanks to poly-cap optics. The spot size varies as a function of the energy, being 17 μm at 2.3 KeV and 32 μm at 18.3 KeV. The focusing process is supported by two video microscopes, one of them explores the sample under a low magnification (1 $cm^2$ area) whereas the other performs the final focusing (1 $mm^2$ area). As the instrument can detect elements with an atomic number (Z) higher than 10 (starting from sodium), the measurements were performed under vacuum (20 mbar) to enhance the detection of the lightest elements. A deconvolution of the signals in the sum spectrum representing the whole mapped area was conducted automatically to construct the elemental images. After that, the distribution map of each element was represented as a function of the intensity of each detected element Kα line, except for Pb, using in this case the Lβ line. The spectra acquisition and the image construction were performed using the M4 TORNADO software.

#### 2.2.2. The Raman spectrometer

Part of the molecular characterization was performed with the Renishaw inVia Raman high resolution micro-Raman spectrometer (Renishaw, UK).The system implements a 532 and 785 nm excitation diode lasers and a charge couple device detector (Peltier cooled). The device was coupled to a confocal microscope with an objective of 20× N PLAN EPI (0.40 NA) to perform microscopic Raman measurements and point-by-point analyses. Acquisition times and number of scans were set to optimize the signal-to-noise ratio. In both cases, the laser power (5–10 % of the total nominal power, which is 100 mW) was modulated to avoid thermal decomposition and chemical or mineralogical transformations. The calibration of this instrument was performed daily with the 520.5 $cm^{-1}$ silicon band. For data analysis and interpretation, WiRE 4.2 software (Renishaw's Windows-based Raman environment) was used. The data analysis, in some cases, consisted of baseline correction to better see the bands of these minerals. In addition, in some other cases, when the bands were broad, it was necessary to decompose these bands into Lorentzian/Gaussian ones, as is the case of kerogen. All collected spectra were compared with pure standard spectra contained in our own spectra databases, the RRUFF™ online database (Lafuente et al., 2015) or bibliography (Freeman et al., 2008; Saikia et al., 2016; Ruiz-Galende et al., 2020a).

#### 2.2.3. The VNIR spectrometer

Other part of the molecular characterization was performed with VNIR spectroscopy, specifically by using the ASD high-resolution FieldSpec4 spectroradiometer (Analytical Spectral Devices Inc., Boulder, USA) equipped with the ASD probe for remote mode operations. The light source consisted of a halogen lamp (ASD Iluminator) placed at 30 cm of distance from the samples. The angle between the incident light and the sample, and that between the sample and the detector fiber was 45° in both cases. The fiber has an acceptance cone with an angle of 25° and was placed to a minimum distance of the sample to minimize the measurement surface. This device works in the 350 to 2500 nm wavelength range and uses three detectors for the different spectroscopic ranges: 350–1000 nm (silicon photodiode array for Vis–NIR), 1001–1800 nm (InGaAs photodiode for SWIR1), and 1801–2500 nm (InGaAs photodiode for SWIR2). The spectral resolution is of 3 nm in the visible region and 6 nm in the near infrared region. Sensor optimization and calibration were set with a Spectralon® white reference scanned once before each sample, and each spectrum is the result of the average of 10 scans. Spectra were collected with RS3 software (ASD Inc.), analyzed with the ViewSpecPro software (ASD Inc.), and compared with those found in the bibliography (Ruiz-Galende et al., 2020a; Clark et al., 2007; Cloutis et al., 2008).

## 3. Results and discussion

As described above, elemental characterization was performed by using μ-EDXRF. Figs. S3 and S4 show the elemental composition of some of the Enekuri analyzed samples, and Figs. S5 and S6 represent the elemental distribution of the Fruiz analyzed samples.

In general terms, the composition of all the analyzed samples was similar. The elements under 1 % *w*/w were considered minor elements and those that were over 1 % w/w were the major elements (Namieśnik, 2002) and the most interesting ones for the molecular characterization. The intensity of the colors in the figures is directly correlated with the relative presence of the element. Thus, the higher color intensity the higher relative presence of each element. In this way and as in the previous cases (Armintza and Meñakoz (Ruiz-Galende et al., 2021; Ruiz-Galende et al., 2020b)), the most concentrated elements were in general, Ca, Si, Fe, Al and Mg, which is in concordance with the molecular characterization as will be described below.

In Fig. S3, one example of the Enekuri samples is shown. As can be seen, Si, Al and K were the most homogeneously distributed elements, which leads to think in the presence of silicates as the most common minerals. Ca, Mn and Sr were the elements found in the white areas of the sample. Ca and Mn had a quite similar elemental distribution, but calcium was supposed to be in the form of carbonate and manganese in the form of some oxide. In the case of Sr, it appeared as an impurity of the calcium carbonate and for that reason they were closely related in all the analyzed samples. Fe, Al, Mg, Ti, V and Co were detected in the same regions of a specific area of the sample. Thanks to the Raman analyses (see below) chlorites and oxides were identified in those areas. Sulfur was found in much localized points and, as in the other emplacements, is related to the presence of sulfides or sulfates.

In Fig. S4, another example of an Enekuri analyzed sample can be seen. The elements distribution was more or less the same as in the previous example. Nevertheless, the only difference was the presence of sodium and phosphorous. In the case of the sodium, this coexisted with aluminum and silicon, which would match with the composition of an aluminosilicate. Regarding to phosphorous, it coexisted with calcium, so it could be related to the presence of apatite ($Ca_5(PO_4)_3(F,Cl,OH)$).

In contrast, Fig. S5 shows the elemental distribution on a Fruiz sample. A homogeneous distribution can be seen in almost all the displayed elements. Si, Al, Fe, Ca, Mg and Na were the most concentrated ones. All of them were supposed to be related to the presence of silicates or carbonates. The minor and trace elements were explained as in the previous cases, except in the case of chromium, which was also identified in Meñakoz (Ruiz-Galende et al., 2020b). It appeared in much localized areas and in very low relative presence, and, unfortunately, it was not possible to detect any mineral by using molecular spectroscopies.

In the following example (Fig. S6), the μ-EDXRF results were very similar to that observed in the previous one. That means that the elements were homogeneously distributed. However, in this case, calcium and sulfur appeared in most localized areas, which was not the case in Fig. S5. These hot spots were analyzed them with the molecular spectroscopies. As in some of the previous cases, these elements were likely related to the presence of carbonates and sulfides/sulfates respectively.

After analyzing the elemental composition of the four samples, the molecular characterization was carried out. In this sense, a small portion of each sample was first ground and analyzed by XRD spectroscopy.

In Enekuri, the main minerals found were quartz and calcite (present in all the measured samples). Other oxides such as anatase, and carbonates, such as dolomite and ankerite, were detected in lower proportions.

Regarding the silicates, the most recurrent ones were micas and plagioclases and the results suggested clinochlore ($Mg_5Al(Si_3Al)O_{10}(OH)_8$) and anorthite ($CaAl_2Si_2O_8$), respectively. In some samples, peaks related with the presence of sanidine ($(K,Na)(Si,Al)_4O_8$), muscovite ($KAl_2(AlSi_3O_{10})(OH)_2$), laumontite ($CaAl_2Si_4O_{12}{\cdot}4H_2O$), and wairakite ($CaAl_2Si_4O_{12}{\cdot}2H_2O$) were found. The latest two belong to the group of the zeolites, which are commonly related to hydrothermal processes that could have occurred in this emplacement. Zeolites, also observed on Mars by TES (Ruff, 2004) and CRISM (Bishop and Michalski, 2017), can easily incorporate a large amount of volatiles. Therefore, their existence on Mars could have important implications for the explanation of the geological history (Cloutis et al., 2002), because they could be an important sink for a variety of Martian volatiles. The identification of these compounds is in agreement with the elemental information obtained by μ-EDXRF for most of the elements.

According to the XRD analyses of Fruiz samples, albite ($NaAlSi_3O_8$), clinochlore, diopside ($CaMgSi_2O_6$) and sanidine were the minerals found in all the samples but in very low concentrations. In addition, in some of the samples quartz was also identified.

The XRD molecular characterization of the samples was completed by means of Raman and VNIR spectroscopies.

One of the most common mineral found by Raman in the analyzed samples, both from Enekuri and Fruiz, was the Na-feldspar, albite ($NaAlSi_3O_8$). It was identified thanks to its Raman bands at 293 (w), 480 (s) and 510 (s) $cm^{-1}$(Fig. 1 a). Taking into account the study made by Freeman et al. (Freeman et al., 2008) these Raman bands correspond to a low ordered albite. This finding was also made in the coastline outcrops, and therefore, its finding in the inland outcrops leads to conclude that they have the same submarine volcanic origin (Ruiz-Galende et al., 2021; Ruiz-Galende et al., 2020b).

Moreover, minerals of the pyroxene group could be identified for the first time in the emplacements studied in this work. Specifically, clinopyroxenes such as diopside ($CaMgSi_2O_6$, Fig. 1 b) was identified thanks to its Raman bands at 326 (m), 360 (w), 392 (m), 666 (s), 860 (w), 1008 (s) and 1158 (w) $cm^{-1}$. This spectrum is very similar to that of augite

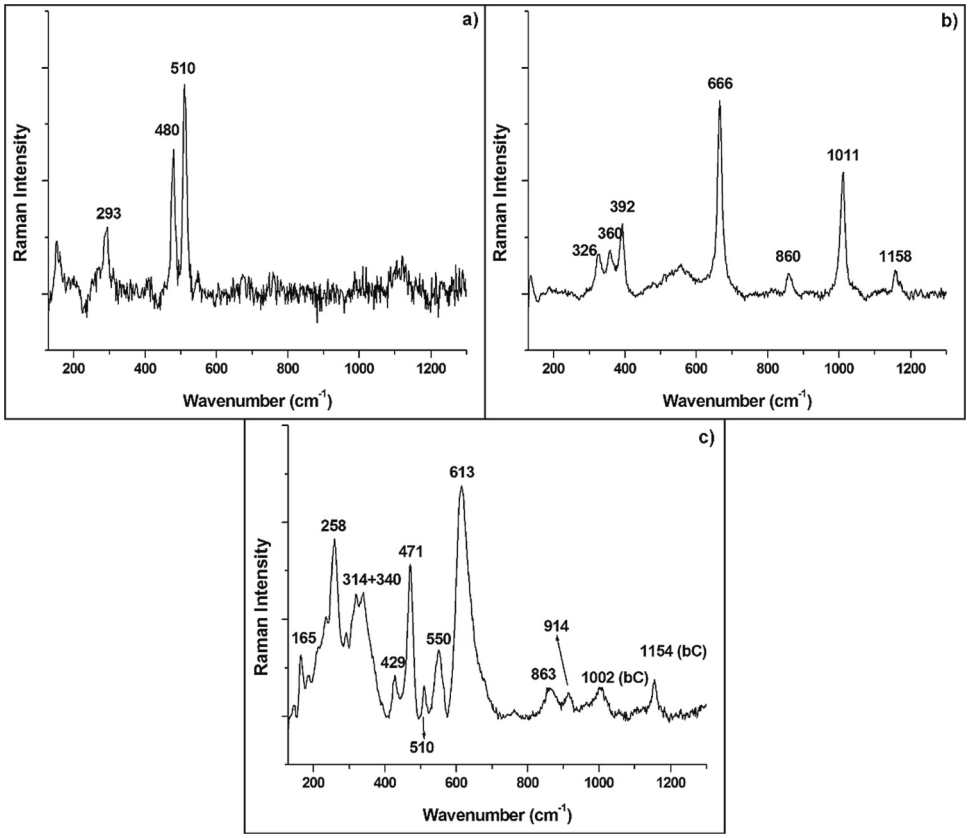


**Fig. 1.** Raman spectra of a) albite, b) diopside and c) titanite together with β-carotenes (bC) found in Enekuri and Fruiz samples.

($(Ca,Mg,Fe)_2(Si, Al)_2O_6$), and therefore, it is difficult to differentiate between them. They are rock-forming ferromagnesian silicates that occur as stable phases in almost every type of igneous rocks. They belong to the inosilicate minerals and, depending on the crystallization system, they are divided into orthopyroxenes and clinopyroxenes (Buchs and Howie, 2016). Moreover, in nature, pyroxenes are often mixtures, which make the differentiation between them even more difficult. Geochemically, the augite series is the most important and its members are the most important constituents of igneous rocks (Huang and Wang, 2005). This finding is relevant because pyroxenes on Mars are present along its entire surface. For example, Bandfield et al. (Ruiz-Galende et al., 2021) demonstrated their presence in Syrtus Major and Achilles et al. (Robles et al., 2014) demonstrated the existence of this type of minerals in Gale crater.

The nesosilicate titanite ($CaTiSiO_5$) was identified by Raman spectroscopy with its bands: 165 (w), 258 (m), 314 and 340 (m), 429 (w), 471 (m), 510 (w), 550 (w), 613 (s), 863 (w) and 914 (w) $cm^{-1}$ (Fig. 1 c). Natural titanite occurs in igneous and metamorphic rocks and the incorporation of trace elements such as U, Th or rare earth elements is very common (Martín-Chivelet et al., 2002). It is an example of an accessory mineral, which could provide insight into the trace-element composition of the rock and, therefore, it helps to address questions about the formation of silicic plutonic and volcanic rocks and how they are related (Ubide Garralda, 2013). To our knowledge, titanite is not reported to be present on Mars, but on Earth, evidences for microbial alteration in subaqueous volcanic rocks where titanite is one of the phases that help in the preservation of bioalteration textures generated by that microbial alteration, have been reported (García-Mondéjar et al., 2019).

In this emplacement, among the most found weathering products, there were chlorites ($(Fe,Mg)_5Al(Si_3Al)O_{10}(OH)_6$), concretely, chamosite (Fe-rich chlorite) and clinochlore (Mg-rich chlorite), as was the case in the coastline outcrops. The Raman bands related to the presence of chamosite are 193 (m) and 366 (w) $cm^{-1}$, and those related to clinochlore are 547 (s) and 679 (s) $cm^{-1}$ (Fig. 2 a).

Chlorites were also identified by means of VNIR (Fig. 2 b and c). Chamosite was found in samples from Enekuri thanks to the bands at 2253 and 2340 nm, which are due to the vibrations of Fe-OH and Mg-OH respectively. Besides, the bands related with the presence of iron were observed at 743, 926 and 1119 nm. In some chamosite spectra (the example of Fig. 2 b), a weak band at 2205 nm can be observed. This band is due to the Al-OH vibration and suggests the presence of the mentioned white micas, such as muscovite or celadonite, which are alteration minerals formed by hydrothermal processes (Gómez Tejedor, 1976; Bustillo, 2003; Rodríguez-Losada et al., 2000).

On the other hand, the spectrum of clinochlore was identified in Fruiz samples (Fig. 2 c) thanks to the bands of the Fe-OH (2295 nm) and Mg-OH (2356 nm) vibrations, which differ slightly from those of chamosite. This group of phyllosilicates comes from the weathering of feldspars (albite) or pyroxenes (diopside), and they are alteration products of Fe- and Mg- bearing minerals. They are common minerals in rocks that have experienced hydrothermal processes (García-Mondéjar et al., 2019), as it could have happened here in the moment of the volcanic eruption.

In Enekuri, prehnite was found by means of Raman spectroscopy (Fig. 3 a) and analcime by means of VNIR spectroscopy (Fig. 3 b). Prehnite ($Ca_2Al(Si_3Al)O_{10}(OH)_2$) is a metamorphic inosilicate hydrothermally formed in basic igneous rocks (Badillo et al., 1987). Its Raman bands appear at 389 (w) and 521 (s) $cm^{-1}$. Analcime ($NaAlSi_2O_6{\cdot}H_2O$) is a zeolite generally formed by reactions between saline solutions and volcanic glass (Castañares et al., 1997). It has VNIR bands at 965, 1158, a doublet at 1421 and 1465 due to the OH vibrations, 1801, 1908 ($H_2O$ combination band), 2117 and 2207 nm. This finding completes the information provided by XRD, where some other zeolites were identified. The zeolites detected by XRD technique were those of calcium, however, as Barth-Wisching et al. (Agirrezabala and García-Mondéjar, 2001) stated, Na-rich zeolites could be formed from Ca-rich ones during their last alteration states when the concentration of Na, the alkalinity and the

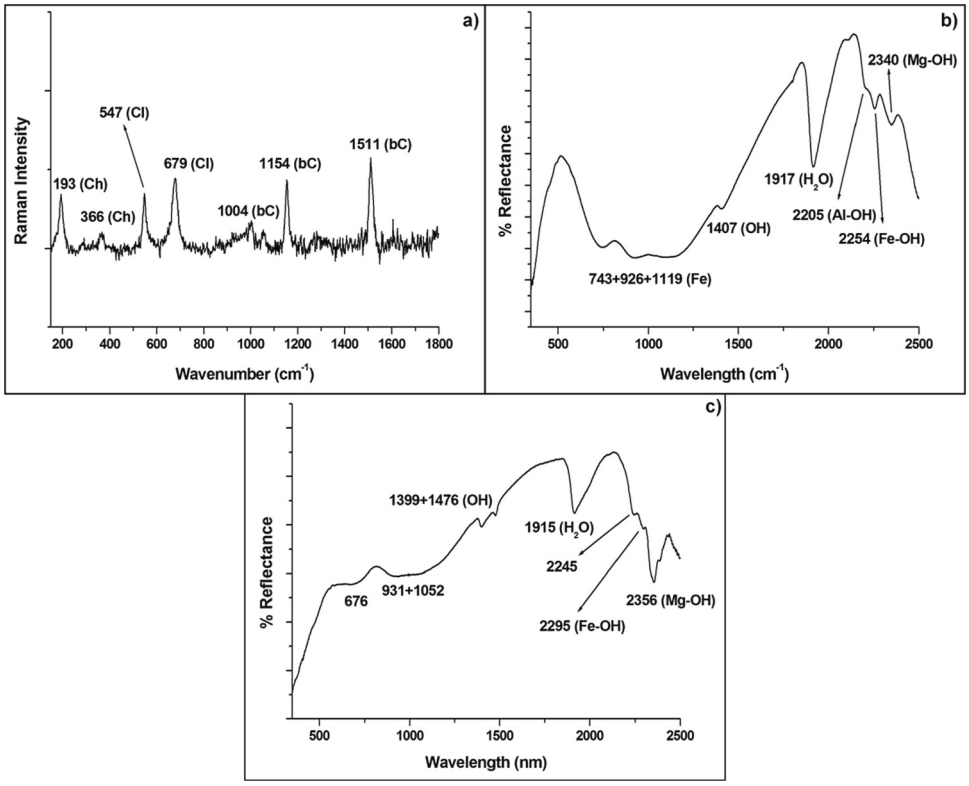


**Fig. 2.** a) Raman spectrum of chamosite (Ch) and clinochlore (Cl) together with β-carotenes (bC), b) VNIR spectrum of chamosite and c) VNIR spectrum of clinochlore.

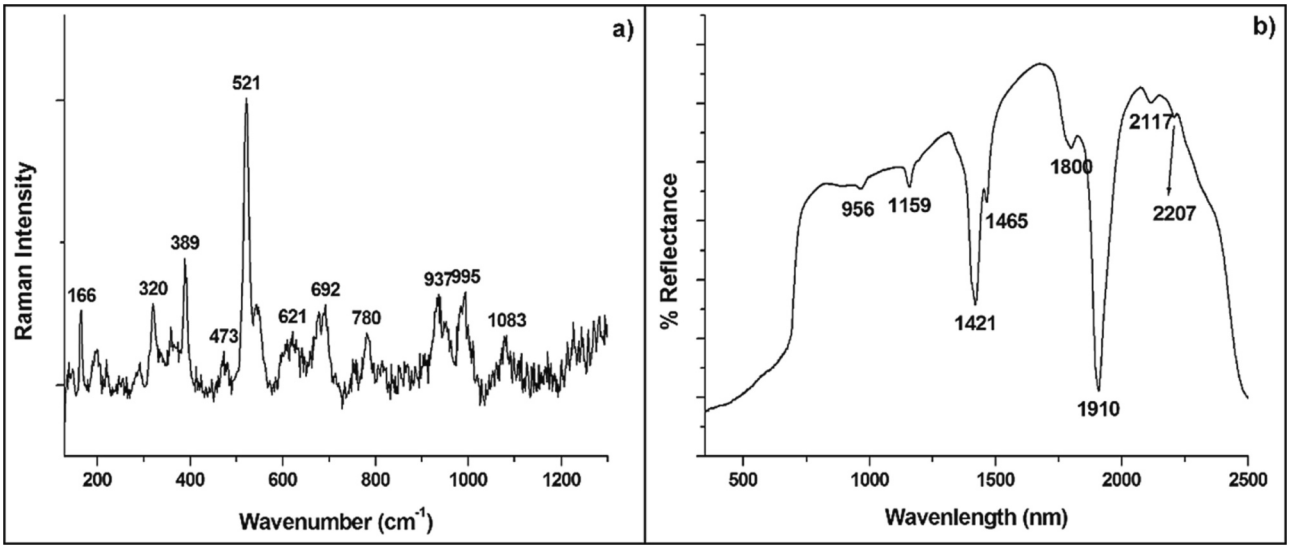


**Fig. 3.** a) Raman spectrum of prehnite and b) VNIR spectrum of analcime.

temperature are the proper ones. The formation of analcime can be due to alteration processes; in a close system by reaction of concentrated alkaline saline solutions (sea-water) at low temperatures, or in an open system by reaction with dilute sodium solutions at elevated temperatures (Barth-Wirsching et al., 1994). On Mars, both minerals are present in Nili Fossae and they were identified by CRISM (Bishop and Michalski, 2017). The presence of prehnite and zeolites (like analcime) in and around the impact crater of the Nili Fossae area are indicators of low grade metamorphic or aqueous hydrothermal alteration (Bishop and Michalski, 2017).

In Fruiz, some oxides were identified. Fig. 4 a, shows a broad Raman band that was decomposed into several bands. These bands at 499, 577, 612 and 654 $cm^{-1}$, are consistent with the presence of manganese oxides. Most of Mn oxides are amorphous and this is the reason why a broad band is observed. These minerals are very reactive and therefore are very important for biogeochemical processes due to their high oxidizing capacity (Cuevas et al., 1981).

Another oxide found in Fruiz is magnesioferrite ($MgFe_2O_4$). It is a spinel, which arise from the second stage of oxidation of olivine, probably present in the original matter from the submarine volcano. This process consists of a first oxidation of the olivine to ferriolivine, and a second one in which the magnesioferrite is formed as a final product (Lafuente et al., 2015). It was identified by the VNIR spectroscopy (Fig. 4 b) and the bands related to this mineral are located at 701 and 1034 nm, which are attributed to the $Fe^{3+}$ intra-atomic transitions (Freeman et al., 2008). In the same Figure, a band consistent with the presence of chamosite can be seen although the number of times that chamosite was detected was much lower than the times that clinochlore (the other chlorite found) was observed. There is no reference confirming the presence of magnesioferrite on Mars, but Zhang et al. (Saikia et al., 2016) found this mineral thanks to high resolution TEM analyses in the Martian meteorite NWA 7755.

Quartz ($SiO_2$) and calcite ($CaCO_3$, Fig. S7) were also detected during the Raman and VNIR spectroscopic analyses. Quartz was found in all the samples from both emplacements throughout the surfaces. In the case of calcite, it was localized in vesicles in the Enekuri samples, as in the case of Meñakoz and Armintza, which evidenced the secondary formation of this mineral and, therefore, the same geological formation, the pillow lavas. However, in the Fruiz samples this carbonate was not found in vesicles, which could be due to the different type of outcrop, a columnar disjunction in this case.

## 4. Conclusions

During the Introduction, it has been stated that the weathering processes that occurred in the analyzed emplacements of this work should be different to those observed in the coastline volcanic outcrops. This statement was confirmed with the obtained results. The only

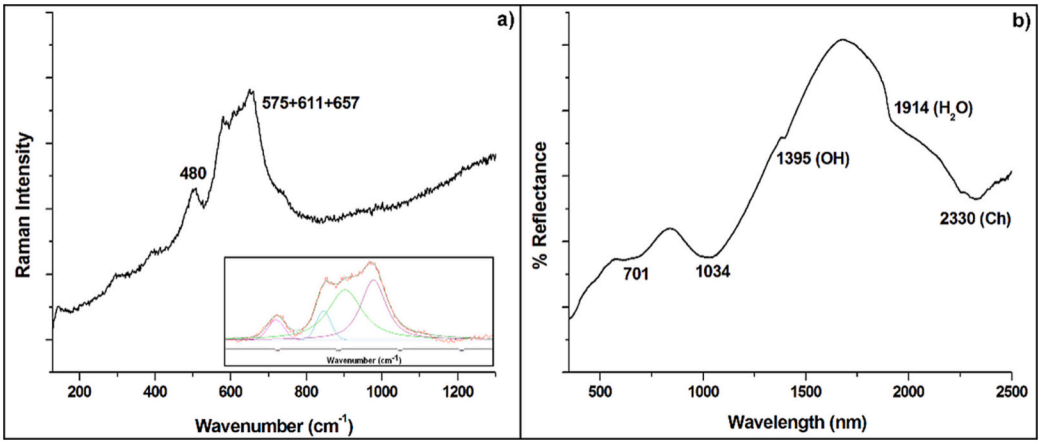


**Fig. 4.** a) Raman spectrum of manganese oxide and b) VNIR spectrum of magnesioferrite together with bands related to the presence of chamosite.

common compounds with these latest emplacements were albite and chlorites. Albite could be formed in aqueous conditions (albitization process) since the geological formations observed in these emplacements have a submarine origin. For their part, chlorites appear as hydrothermal products, which is in agreement with the mentioned formations.

However, the lack of contact with sea-water since 50 My until nowadays led us to conclude that the environmental transformation of these minerals had to be different since the compounds observed in the samples from Enekuri and Fruiz outcrops are different from those observed in coastline outcrops. The existence of pyroxenes in the analyzed samples could lead to the conclusion that the weathering process did not progress as much as in the emplacements in contact with the sea-water. This could be also the case of the titanite, which has magmatic origin and has commonly been reported to be altered to anatase (Ruiz-Galende et al., 2020a), among other oxides whose presence was not as evident as in the coastline outcrops. Moreover, due to the existence of titanite, both Enekuri and Fruiz could be considered good examples for the studies of biological activity and the possible implication with Mars.

The presence of chlorites indicates that the first steps of the weathering process should be similar to those observed in the previous studied emplacements. Moreover, the hydrothermal origin of these minerals is consistent with the submarine volcanic origin of the analyzed areas.

However, there are also differences observed between Enekuri and Fruiz, which could be related to the geological feature observed (pillow lavas and columnar disjunction) or with the different plates in which they are present (Iberian and European respectively). In Enekuri, prehnite and analcime, and in Fruiz, manganese oxides and magnesioferrite are supposed to be minerals that arose in the first steps of the weathering process because, if not, they would have been observed in the coastline outcrops too.

## CRediT authorship contribution statement

**Jennifer Huidobro:** Contextualization, Methodology, Formal analysis, Investigation, Data Curation, Writing – Original Draft, Writing – Review and Editing, Visualization, Project Administration. **Patricia Ruiz-Galende:** Contextualization, Methodology, Formal analysis, Investigation, Data Curation, Writing – Original Draft, Visualization, Project Administration. **Imanol Torre-Fdez:** Conceptualization, Methodology. **Julene Aramendia:** Validation, Writing – Review and Editing. **Jesús Martínez-Frías:** Validation. **Cristina García-Florentino:** Conceptualization, Methodology, Validation. **Leticia Gómez-Nubla:** Conceptualization, Validation. **Kepa Castro:** Validation, Investigation, Data Curation, Supervision, Writing – Review and Editing. **Gorka Arana:** Validation, Investigation, Data Curation, Supervision, Writing – Review and Editing. **Juan Manuel Madariaga:** Conceptualization, Validation, Investigation, Data Curation, Supervision, Writing – Review and Editing, Funding Acquisition.

## Declaration of competing interest

The authors declare the following financial interests/personal relationships which may be considered as potential competing interests: Juan Manuel Madariaga reports financial support was provided by Spanish Agency for Research. Juan Manuel Madariaga reports were provided by University of the Basque Country.

## Data availability

Data will be made available on request.

## Acknowledgements

This work has been supported through the PAMMAT project "Alteration processes in Mars and Moon Meteorites, and Terrestrial Analogues at different environments: Mars2020, Rosalind Franklin and Returned Samples from Mars and Moon" (Grant No. PID2022-142750OB-I00), funded by the Spanish Agency for Research (through the Spanish Ministry of Science and Innovation, MICINN, and the European Regional Development Fund, FEDER), and the Strategic Project "Study of Alteration Processes in Terrestrial and Planetary Materials" (Grant No. UPV/EHU PES21/88), funded by the UPV/EHU.

J. Huidobro is grateful to the Basque Government for her pre-doctoral contract (Ref. PRE_2022_2_0089). P. Ruiz-Galende and I. Torre-Fdez are grateful to the UPV/EHU for their pre-doctoral. J. Aramendia and C. García-Florentino thank their post-doctoral contracts from the UPV/EHU and the Basque Government respectively.

## Appendix A. Supplementary data

Supplementary data to this article can be found online at https://doi.org/10.1016/j.scitotenv.2023.167186.

## References

Agirrezabala, L.M., García-Mondéjar, J., 2001. Kinematic indicators and mineralization on the Elgoibar Faul (Basque-Cantabrian Basin). Geogaceta 30, 7–10.
Badillo, J., Orue-Etxebarria, X., Radríguez, J., 1987. Las Facies Supraurgonianas Entre La Avanzada y El Puente de Rontegi (Bizkaia), Son de Edad Albiniense Superior. In: Estud. del Inst. Alavés la Nat, 2, pp. 171–177.
Barth-Wirsching, U., Klammer, D., Kovic-Kralj, P., 1994. The formation of analcime from laumontite in the Smrekovec Volcanics, Northwest Slovenia - an experimental approach. Stud. Surf. Sci. Catal. 84, 299–305. https://doi.org/10.1016/S0167-2991(08)64127-0.
Carter, J., 2017. In: Bishop, J.L., Michalski, J.R., Gates, W., Kloprogge, J.T., Madejova, J., Bergaya, F. (Eds.), Remote Detection of Clay Minerals, Infrared and Raman Spectroscopies of Clay Minerals. Elsevier, pp. 482–514. https://doi.org/10.1016/B978-0-08-100355-8.00014-X.
Buchs, D.M., Howie, R.A., 2016. Pyroxenes. In: Elias, S.A. (Ed.), Reference Module in Earth Systems and Environmental Sciences. Elsevier, pp. 1–4. https://doi.org/10.1016/B978-0-12-409548-9.09697-4.
Bustillo, M., 2003. Green opals in hydrothermalized basalts (Tenerife Island, Spain): alteration and aging of silica pseudoglass. J. Non-Cryst. Solids 323 (1–3), 27–33. https://doi.org/10.1016/S0022-3093(03)00288-6.
Castañares, L.M., Robles, S., Vicente Bravo, J.C., 1997. Distribución Estratigráfica de Los Episodios Volcánicos Submarinos Del Albiense-Santoniense En La Cuenca Vasca (Sector Gernika-Plentzia, Bizkaia). Geogaceta 22, 43–46.
Clark, R.N., Swayze, G.A., Wise, R.A., Livo, K.E., Hoefen, T.M., Kokaly, R.F., Sutley, S.J., 2007. USGS Digital Spectral Library Splib06a. In: Digital Series 231, Vol. 231. https://doi.org/10.3133/ds231.
Cloutis, E.A., Asher, P.M., Mertzman, S.A., 2002. Pyroxene reflectance spectra: minor absorption bands and effects of elemental substitutions. J. Geophys. Res. 107 (E6), 5039. https://doi.org/10.1029/2001JE001590.
Cloutis, E.A., Craig, M.A., Kruzelecky, R.V., Jamroz, W.R., Scott, A., Hawthorne, F.C., Mertzman, S.A., 2008. Spectral reflectance properties of minerals exposed to simulated Mars surface conditions. Icarus 195, 140. https://doi.org/10.1016/j.icarus.2007.10.028.
Cuevas, J., Garrot, A., Tubia, J.M., 1981. Análisis y Significado de Diferentes Tipos de Estructuras En El Magmatismo Del Cretacico Superior de La Cuenca Vasco-Cantábrica (1.ª Parte). Munibe. Soc. Ciencias ARANZADI, 33 (1–2), pp. 1–20.
Freeman, J.J., Wang, A., Kuebler, K.E., Jolliff, B.L., Haskin, La A., 2008. Characterization of natural feldspars by Raman spectroscopy for future planetary exploration. Can. Mineral. 46, 1477. https://doi.org/10.3749/canmin.46.6.1477.
García-Mondéjar, J., Carracedo-Sánchez, M., Owen, H.G., Fernández-Mendiola, P.A., 2019. The early Aptian volcanic episode of Gutiolo (N Spain): expression of the Bilbao Rift Fault Zone. Geol. J. 54 (6), 3509–3526. https://doi.org/10.1002/gj.3342.
Gómez Tejedor, J., 1976. Historia Geológica de Vizcaya. Caja de ahorros Vizcaína, Bilbao, Spain.
Goudge, T.A., Mustard, J.F., Head, J.W., Fassett, C.I., Wiseman, S.M., 2015. Assessing the mineralogy of the watershed and fan deposits of the Jezero crater paleolake system, Mars. J. Geophys. Res. Planets 120 (4), 775–808. https://doi.org/10.1002/2014JE004782.
Head, J.W., 2007. In: Chapman, M. (Ed.), The Geology of Mars: New Insights and Outstanding Questions, The Geology of Mars. Cambridge University Press, New York, p. 12. https://doi.org/10.1017/CBO9780511536014.002.
Huang, P.M., Wang, M.K., 2005. In: Hillel, D. (Ed.), Minerals, Primary, Encyclopedia of Soils in the Environment. Elsevier, Oxford, UK, pp. 500–510.
Lafuente, B., Downs, R.T., Yang, H., Stone, N., 2015. The power of databases: the RRUFF Project. In: Armsbruster, T., Danisi, R.M. (Eds.), Highlights in Mineralogical Crystallography. De Gruyter, Berlin, Germany, pp. 1–30.
Martín-Chivelet, J., Berásategui, X., Rosales, I., Vilas, L., Vera, J.A., Caus, E., Gräfe, K.U., Mas, R., Puig, C., Segura, M., Robles, S., Floquet, M., Quesada, S., Ruiz-Ortiz, P.A., Fregenal-Martínez, M.A., Salas, R., Arias, C., García, Á., Martín-Algarra, A.,

Meléndez, M.N., Chacón, B., Molina, J.M., Sanz, J.L., Castro, J.M., García-Hernández, M., Carenas, B., García-Hidalgo, J., Gil, J., Ortega, F., 2002. Cretaceous. In: Gibbons, W., Moreno, T., London, G. S. of (Eds.), The Geology of Spain. The Geological Society, London, UK, p. 255. https://doi.org/10.1144/GOSPP.12.

Namieśnik, J., 2002. Trace analysis — challenges and problems. Crit. Rev. Anal. Chem. 32 (4), 271–300. https://doi.org/10.1080/10408340290765579.

Reyes Ayala, K.I., 2016. Análisis Geológico de La Región Oxia Planum En Marte, Sitio Principal de Aterrizaje de La Misión ExoMars 2020. Universidad Nacional Autonómica de México, México.

Robles, S., Aranburu, A., La Apraiz, A., 2014. Cuencia Vasco-Cantábrica: Génesis y Evolución Tectosedimentaria. In: Rev. la Asoc. Española para la Enseñanza las Ciencias la Tierra, 22 (2), pp. 99–144.

Rodríguez-Losada, J., Martinez-Frias, J., Bustillo, M., Delgado, A., Hernandez-Pacheco, A., de la Fuente Krauss, J., 2000. The hydrothermally altered ankaramite basalts of Punta Poyata (Tenerife, Canary Islands). J. Volcanol. Geotherm. Res. 103 (1–4), 367–376. https://doi.org/10.1016/S0377-0273(00)00231-6.

Ruff, S.W., 2004. Spectral evidence for zeolite in the dust on Mars. Icarus 168 (1), 131–143. https://doi.org/10.1016/j.icarus.2003.11.003.

Ruiz-Galende, P., Torre-Fdez, I., Aramendia, J., Gomez-Nubla, L., Castro, K., Arana, G., Vallejuelo, S.F., Maguregui, M., Medina, J., Baonza, V.G., Rull, F., Madariaga, J.M., 2020a. New Raman–visible near-infrared database of inorganic and mineralogical planetary and terrestrial compounds and its implications for Mars: phyllosilicates. J. Raman Spectrosc. 51, 1750. https://doi.org/10.1002/jrs.5677.

Ruiz-Galende, P., Torre-Fdez, I., Aramendia, J., Gómez-Nubla, L., Castro, K., Arana, G., Madariaga, J.M., 2020b. Study of a terrestrial Martian analogue: geochemical characterization of the Meñakoz outcrops (Biscay, Spain). J. Raman Spectrosc. 51 (9), 1603–1612. https://doi.org/10.1002/jrs.5565.

Ruiz-Galende, P., Fernández, G., Torre-Fdez, I., Aramendia, J., Gomez-Nubla, L., García-Florentino, C., Castro, K., Arana, G., Madariaga, J.M., 2021. Characterization of sedimentary and volcanic rocks in Armintza Outcrop (Biscay, Spain) and its implication for Oxia Planum (Mars) exploration. Spectrochim. Acta A Mol. Biomol. Spectrosc. 251, 119443. https://doi.org/10.1016/j.saa.2021.119443.

Saikia, B.J., Parthasarathy, G., Borah, R.R., Borthakur, R., 2016. Raman and FTIR spectroscopic evaluation of clay minerals and estimation of metal contaminations in natural deposition of surface sediments from Brahmaputra River. Int. J. Geosci. 7 (7), 873–883. https://doi.org/10.4236/ijg.2016.77064.

Sutter, B., Dalton, J.B., Ewing, S.A., Amundson, R., McKay, C.P., 2007. Terrestrial analogs for interpretation of infrared spectra from the martian surface and subsurface: sulfate, nitrate, carbonate, and phyllosilicate-bearing Atacama Desert soils. J. Geophys. Res. Biogeosci. 112, 1. https://doi.org/10.1029/2006JG000313. G04S10.

Torre-Fdez, I., García-Florentino, C., Huidobro, J., Coloma, L., Ruiz-Galende, P., Aramendia, J., Castro, K., Arana, G., Madariaga, J.M., 2021. Characterization of Olivines and Their Metallic Composition: Raman Spectroscopy Could Provide an Accurate Solution for the Active and Future Mars Missions. In: EPCS92021, Vol. 15. #586.

Ubide Garralda, T., 2013. The Cretaceous Alkaline Magmatism in Northeast Iberia: Igneous Processes and Geodynamic Implications. University of Zaragoza, Spain.

Vago, J.L., Westall, F., Pasteur Instrument Teams, L.S., Coates, A.J., Jaumann, R., Korablev, O., Ciarletti, V., Mitrofanov, I., Josset, J.-L., De Sanctis, M.C., Bibring, J.-P., Rull, F., Goesmann, F., Steininger, H., Goetz, W., Brinckerhoff, W., Szopa, C., Raulin, F., Westall, F., Edwards, H.G.M., Whyte, L.G., Fairén, A.G., Bibring, J.-P., Bridges, J., Hauber, E., Ori, G.G., Werner, S., Loizeau, D., Kuzmin, R.O., Williams, R. M.E., Flahaut, J., Forget, F., Vago, J.L., Rodionov, D., Korablev, O., Svedhem, H., Sefton-Nash, E., Kminek, G., Lorenzoni, L., Joudrier, L., Mikhailov, V., Zashchirinskiy, A., Alexashkin, S., Calantropio, F., Merlo, A., Poulakis, P., Witasse, O., Bayle, O., Bayón, S., Meierhenrich, U., Carter, J., García-Ruiz, J.M., Baglioni, P., Haldemann, A., Ball, A.J., Debus, A., Lindner, R., Haessig, F., Monteiro, D., Trautner, R., Voland, C., Rebeyre, P., Goulty, D., Didot, F., Durrant, S., Zekri, E., Koschny, D., Toni, A., Visentin, G., Zwick, M., van Winnendael, M., Azkarate, M., Carreau, C., the ExoMars Project Team, 2017. Habitability on early mars and the search for biosignatures with the ExoMars Rover. Astrobiology 17, 471. https://doi.org/10.1089/ast.2016.1533.

Werner, S.C., 2009. The global Martian volcanic evolutionary history. Icarus 201 (1), 44–68. https://doi.org/10.1016/j.icarus.2008.12.019.